

Instability of radiation-induced flow in an inclined slot

WEN-MEI YANG and MOU-CHANG LEU

Department of Mechanical Engineering, National Chiao Tung University, Hsinchu, Taiwan 30049, R.O.C.

(Received 20 July 1992 and in final form 7 December 1992)

Abstract—The instability of radiation-induced flow of a participating fluid in an inclined slender slot irradiated from one boundary is studied numerically for the inclination from 0° to 90° . The Eddington approximation is employed for the equation of transfer, and the pseudospectral method is used to solve the linearized perturbed equations. At an angle smaller than the transition angle the instability sets in as stationary longitudinal rolls. At an angle greater than the transition angle the instability occurs in the form of travelling transverse waves. The transition angle for the fluid of $Pr = 0.71$ is found to be minimum at the optical thickness near unity. Increasing optical thickness decreases the penetration of radiant energy, consequently increases the stability. The critical Rayleigh number increases rapidly with increasing the optical thickness as the optical thickness is greater than one.

INTRODUCTION

NATURAL convection in an inclined slot driven by a temperature difference between the sidewalls has been noticed for a long period because of its importance in the fundamentals of heat transfer and in applications in this field. When the temperature difference is small the flow is said to be in the conduction regime, for then heat transfer across the slot is primarily by conduction. At a larger temperature difference, an instability sets in either as stationary longitudinal rolls with axes parallel with the direction of mean flow at smaller inclination angle, or as travelling transverse rolls with axes perpendicular to the mean flow at larger inclination angle. Convection becomes the dominant mode of heat transfer after the instability sets in. The stability of flow in the conduction regime was considered by many investigators [1–7] over the last few decades. However, the study of instability of the roll-shape flow in the convection regime is rarely seen. Recently, Clever and Busse [8] investigated the instabilities of longitudinal rolls in an inclined slot. Chait and Korpela [9] considered the stability of the secondary flow in a vertical slot.

The effect of radiation on the flow in an inclined slot is of interest in material processing and in solar collector applications. Arpaci and Bayazitoglu [10], Hassab and Ozisik [11] examined the effects of radiation parameters on the stability of flow in the conduction regime. They found that radiation has a stabilizing effect on the onset of roll-shape flow.

Radiation-induced natural convection has received attention in atmospheric science and was noticed recently in some new technologies such as laser fusion. Webb and Viskanta [12] experimentally studied the natural convection in a vertical rectangular enclosure heated by irradiation from one side. Yang [13] considered the stability of a horizontal fluid layer

irradiated from the top. In this paper, the stability of radiation-induced flow in the conduction regime in an inclined slot is studied. Both longitudinal and transverse mode of disturbances are considered. The effects of inclination angle and some radiation parameters are presented.

FORMULATION

Consider a layer of fluid of thickness L contained inside a slot, which is inclined from the horizontal by an angle ϕ , as shown in Fig. 1. A radiative heat flux q'' is incident upon the upper surface, which has a hemispherical total reflectivity and transmissivity Γ and $1 - \Gamma$, respectively, and a convective heat transfer coefficient h with the surrounding which is at the temperature T_∞ . For a participating fluid, the in-

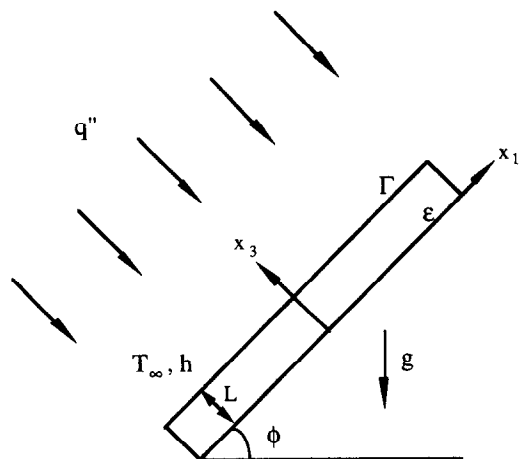


FIG. 1. An inclined slot.

NOMENCLATURE

Bi	Biot number	γ_1	constant
C	$(\partial\bar{p}/\partial x_1) + (\rho_\infty L^3/\mu\alpha)g \sin \phi$	γ_2	constant
E_b	blackbody emissive power	ε	emissivity of the lower plate
g	gravity	ζ	coordinate for Chebyshev polynomials
h	convective heat transfer coefficient	η	nongrayness
J	magnitude of the disturbance of j	Θ	magnitude of the disturbance of temperature
j	zeroth moment of radiative intensity	θ	temperature
k	wavenumber	κ	thermal conductivity
L	thickness of the inclined slot	λ_i	unit vector, $(-\sin \phi, 0, -\cos \phi)$
P	Planck number; magnitude of the disturbance of p	μ	dynamic viscosity
p	pressure	ν	kinematic viscosity
Pr	Prandtl number	ρ	density
q_i^R	radiative heat fluxes	σ	Stefan-Boltzmann constant or growth rate of the disturbances
q''	irradiation	τ	optical thickness
Ra	Rayleigh number	ϕ	inclination angle
T	dimensional temperature	ϕ_i	transition angle
T_n	n th degree of Chebyshev polynomial	ψ	stream function
t	time	ω	albedo.
W	magnitude of the disturbance of velocity		
v_i	velocities		
x_i	coordinates.		
Greek symbols		Superscript	
α	thermal diffusivity	—	basic state.
α_p	Planck mean absorption coefficient	Subscripts	
α_R	Rosseland mean absorption coefficient	c	critical value
Γ	transmissivity of the upper surface	∞	surrounding.

coming radiative energy will be absorbed partly by the fluid and partly by the lower solid boundary, which is assumed to be insulated and has the hemispherical total emissivity and reflectivity ε and $1-\varepsilon$, respectively. Consequently, a temperature gradient is developed in the fluid layer. For a small temperature gradient, a unicellular buoyancy driven flow in the slot can be considered one-dimensional in the core region if the aspect ratio of the slender slot is very large. Heat transfer across the slot is primarily by both conduction and radiation. When the temperature gradient is large enough, instability sets in and the flow becomes two-dimensional. Convection then becomes an important mode of heat transfer.

For the incompressible fluid with constant viscosity and conductivity, using the Eddington approximation for the equation of transfer, the equations governing the flow [13, 14] can be written by

$$\frac{\partial v_j}{\partial x_j} = 0 \quad (1)$$

$$\frac{1}{Pr} \left(\frac{\partial v_i}{\partial t} + v_j \frac{\partial v_i}{\partial x_j} \right) = \frac{\rho L^3}{\mu\alpha} g \lambda_i - \frac{\partial p}{\partial x_i} + \frac{\partial^2 v_i}{\partial x_j \partial x_j} \quad (2)$$

$$\frac{\partial \theta}{\partial t} + v_j \frac{\partial \theta}{\partial x_j} = \frac{\partial^2 \theta}{\partial x_j \partial x_j} - \frac{\partial q_i^R}{\partial x_i} \quad (3)$$

$$\frac{\partial^2 q_i^R}{\partial x_j \partial x_j} - \frac{3\tau^2}{1-\omega} q_i^R = 4\eta\tau \frac{\partial E_b}{\partial x_i} \quad (4a)$$

$$\frac{\partial^2 j}{\partial x_j \partial x_j} - \frac{3\tau^2}{1-\omega} j = -12 \frac{\tau^2}{1-\omega} E_b. \quad (4b)$$

In equations (1)–(4) x_i are nondimensionalized by L , v_i by α/L , θ by $q''L/\kappa$, t by L^2/α , p by $\mu\alpha/L^2$, q_i^R , j and E_b by q'' , $\lambda_i = (-\sin \phi, 0, -\cos \phi)$, α is the thermal diffusivity, κ the thermal conductivity, ρ the density, ν and μ the kinematic and the dynamic viscosity respectively, and $Pr = \nu/\alpha$ the Prandtl number. Equation (4a) describes the behavior of the radiative heat fluxes q_i^R , which are also called the first moment of radiative intensity and usually applied for one-dimensional problem. Equation (4b) describes the behavior of the zeroth moment of radiative intensity, which is proportional to the radiative internal energy, and is applicable for multidimensional problem. In both equations $\tau = (\alpha_p \alpha_R)^{1/2} L$ is called the optical thickness, α_p and α_R are the Planck and Rosseland mean absorption coefficients respectively, $\eta = (\alpha_p/\alpha_R)^{1/2}$ the nongrayness, ω the albedo, and E_b the blackbody emissive power.

On the boundaries the following conditions are satisfied.

At $x_3 = 0$:

$$v_1 = v_2 = v_3 = 0 \quad (5a)$$

$$-\frac{\partial \theta}{\partial x_3} + q_3^R = 0 \quad (5b)$$

$$\frac{1}{\eta\tau} \frac{\partial q_3^R}{\partial x_3} - \frac{1}{\gamma_1} q_3^R = 0 \quad (5c)$$

$$\frac{\eta(1-\omega)}{3\tau\gamma_1} \frac{\partial j}{\partial x_3} - j = -4E_b, \quad (5d)$$

At $x_3 = 1$:

$$v_1 = v_2 = v_3 = 0 \quad (5e)$$

$$-\frac{\partial \theta}{\partial x_3} = Bi(\theta - \theta_\infty) \quad (5f)$$

$$\frac{1}{\eta\tau} \frac{\partial q_3^R}{\partial x_3} + \frac{1}{\gamma_2} q_3^R = 4[(E_b - E_{b\infty}) - 1] \quad (5g)$$

$$\frac{\eta(1-\omega)}{3\tau\gamma_2} \frac{\partial j}{\partial x_3} + j = 4(E_{b\infty} + 1) \quad (5h)$$

where $Bi = hL/\kappa$ is the Biot number,

$$\frac{1}{\gamma_1} = 4 \left(\frac{1}{\varepsilon} - \frac{1}{2} \right),$$

 ε is the hemispherical total emissivity of the lower plate, and

$$\frac{1}{\gamma_2} = 4 \left(\frac{1}{\Gamma} - \frac{1}{2} \right),$$

 Γ is the hemispherical total transmissivity of the upper surface.

BASIC FLOW

In the basic state, the flow is one-dimensional. If the fluid satisfies the Boussinesq approximation, by linearizing the emissive power, equations (2), (3) and (4a) can be simplified as

$$\frac{d^2 \bar{v}_1}{dx_3 dx_3} + Ra(\bar{\theta} - \theta_\infty) \sin \phi = C \quad (6)$$

$$\frac{d^2 \bar{\theta}}{dx_3 dx_3} - \frac{d\bar{q}_3^R}{dx_3} = 0 \quad (7)$$

$$\frac{d^2 \bar{q}_3^R}{dx_3 dx_3} - \frac{3\tau^2}{1-\omega} \bar{q}_3^R = 4\eta\tau P \frac{d\bar{\theta}}{dx_3} \quad (8)$$

where $Ra = (g\beta L^3/\nu\alpha)(q''L/\kappa)$ is the Rayleigh number, β is the thermal expansion coefficient, and $P = 4\sigma T_\infty^3/(\kappa/L)$ is the Planck number, which physically represents the ratio of radiation to conduction heat transfer across the slot, σ being the Stefan-Boltzmann constant. The boundary conditions are:

At $x_3 = 0$:

$$\bar{v}_1 = 0 \quad (9a)$$

$$-\frac{d\bar{\theta}}{dx_3} + \bar{q}_3^R = 0 \quad (9b)$$

$$\frac{1}{\eta\tau} \frac{d\bar{q}_3^R}{dx_3} - \frac{1}{\gamma_1} \bar{q}_3^R = 0, \quad (9c)$$

At $x_3 = 1$:

$$\bar{v}_1 = 0 \quad (9d)$$

$$-\frac{d\bar{\theta}}{dx_3} = Bi(\bar{\theta} - \theta_\infty) \quad (9e)$$

$$\frac{1}{\eta\tau} \frac{d\bar{q}_3^R}{dx_3} + \frac{1}{\gamma_2} \bar{q}_3^R = 4[P(\bar{\theta} - \theta_\infty) - 1]. \quad (9f)$$

Although the above equations are somewhat lengthy, they are linear and can be solved in a straightforward manner. The temperature and the radiative heat flux are firstly assumed to be

$$\bar{\theta} - \theta_\infty = C_1 + C_2 \cosh(mx_3) + C_3 \sinh(mx_3), \quad (10)$$

$$\bar{q}_3^R = mC_3 \cosh(mx_3) + mC_2 \sinh(mx_3) \quad (11)$$

where $m = [3\tau^2/(1-\omega) + 4\eta\tau P]^{1/2}$. C_1 , C_2 and C_3 can be found without difficulty from the boundary conditions. They are

$$C_1 = 4 \left[\left(\frac{m^2}{\eta\tau} + \frac{Bi}{\gamma_1} \right) \cosh m + m \left(\frac{Bi}{\eta\tau} + \frac{1}{\gamma_1} \right) \sinh m \right] / \Delta$$

$$C_2 = -\frac{4Bi}{\gamma_1} / \Delta$$

$$C_3 = -\frac{4m Bi}{\eta\tau} / \Delta$$

where

$$\Delta = \frac{m^2}{\eta\tau} \left(4P + \frac{Bi}{\gamma_1} + \frac{Bi}{\gamma_2} \right) \cosh m + m \left(\frac{Bi}{\gamma_1\gamma_2} + \frac{Bi m^2}{\eta^2\tau^2} + \frac{4P}{\gamma_1} \right) \sinh m.$$

Once the temperature distribution is obtained, the velocity can be found from equation (6) by integration twice,

$$\bar{v}_1 = C \frac{x_3^2}{2} - \left[C_1 \frac{x_3^2}{2} + C_2 \frac{\cosh(mx_3)}{m^2} + C_3 \frac{\sinh(mx_3)}{m^2} \right] Ra \sin \phi + C_4 x_3 + C_5. \quad (12)$$

C_4 and C_5 can be found from the boundary conditions and are

$$C_4 = \left(\frac{C_1}{2} + C_2 \frac{\cosh m - 1}{m^2} + C_3 \frac{\sinh m}{m^2} \right) Ra \sin \phi - \frac{C}{2},$$

$$C_5 = C_2 \frac{Ra \sin \phi}{m^2}.$$

The constant C can be determined from the requirement of mass balance,

$$\int_0^1 \bar{v}_1(x_3) dx_3 = 0. \tag{13}$$

Therefore,

$$C = \left[C_1 + C_2 \left(\frac{6 \cosh m + 6}{m^2} - \frac{12 \sinh m}{m^3} \right) + C_3 \left(\frac{6 \sinh m}{m^2} + \frac{12 - 12 \cosh m}{m^3} \right) \right] Ra \sin \phi.$$

The effects of radiation on the basic flow can be found from the above solutions. Temperature distributions for various Biot numbers at different optical thicknesses can be seen from ref. [13]. The velocity distribution of the basic flow at different optical thicknesses for $Ra = 1000$, $Pr = 0.71$, $Bi = 1$, $P = 1$, $\eta = 1$, $\omega = 0$, $\varepsilon = 1$, $\Gamma = 1$ and $\phi = 90^\circ$ is shown in Fig. 2. It is seen that increasing the optical thickness retards radiant energy penetration to the lower boundary, which in turn decreases the velocity of the flow. It is also noted that the antisymmetric velocity, which appears when both boundaries are fixed at different temperatures, no longer exists because of the asymmetric boundary conditions in the present study.

LINEAR STABILITY ANALYSIS

When the incoming radiant energy is greater than a certain amount, the conduction regime may no longer exist. The disturbances grow if the basic state is unstable or decay if stable. In the linear stability analysis, the perturbed quantities are added to the basic

state and then all nonlinear terms are neglected. The equations describing the perturbed quantities, for which the same symbols as in equations (1)–(4) are used, may be written as

$$\frac{\partial v_1}{\partial x_1} + \frac{\partial v_2}{\partial x_2} + \frac{\partial v_3}{\partial x_3} = 0 \tag{14}$$

$$\frac{1}{Pr} \left(\frac{\partial v_1}{\partial t} + \bar{v}_1 \frac{\partial v_1}{\partial x_1} + v_3 \frac{d\bar{v}_1}{dx_3} \right) = - \frac{\partial p}{\partial x_1} + \nabla^2 v_1 + Ra \theta \sin \phi \tag{15a}$$

$$\frac{1}{Pr} \left(\frac{\partial v_2}{\partial t} + \bar{v}_1 \frac{\partial v_2}{\partial x_1} \right) = - \frac{\partial p}{\partial x_2} + \nabla^2 v_2 \tag{15b}$$

$$\frac{1}{Pr} \left(\frac{\partial v_3}{\partial t} + \bar{v}_1 \frac{\partial v_3}{\partial x_1} \right) = - \frac{\partial p}{\partial x_3} + \nabla^2 v_3 + Ra \theta \cos \phi \tag{15c}$$

$$\frac{\partial \theta}{\partial t} + \bar{v}_1 \frac{\partial \theta}{\partial x_1} + \frac{d\bar{\theta}}{dx_3} v_3 = \nabla^2 \theta + \eta \tau (j - 4P\theta) \tag{16}$$

$$\nabla^2 j - \frac{3\tau^2}{1-\omega} j = - \frac{12\tau^2}{1-\omega} P\theta \tag{17}$$

where ∇^2 denotes the three-dimensional Laplacian operator.

Squire's theorem which reduces a three-dimensional stability problem to an equivalent two-dimensional one, is not valid for this system. Hence, three-dimensional disturbances are considered and the perturbed quantities can be written in the form

$$\phi(x_1, x_2, x_3, t) = \Phi(x_3) \exp [i(k_1 x_1 + k_2 x_2) + \sigma t] \tag{18}$$

where $\phi = v_i, p, \theta$ or j , $\Phi = U, V, W, P, \Theta$ or J , and k_1 and k_2 are the wavenumbers of the disturbances in

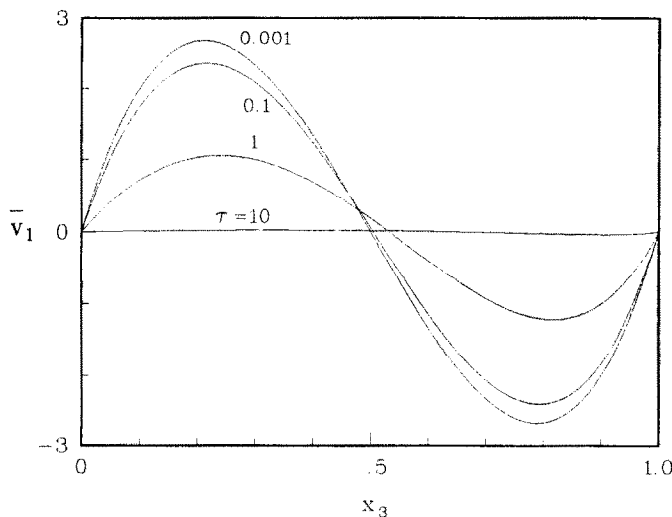


FIG. 2. Velocity distribution of the basic flow at different optical thicknesses for $Ra = 1000$, $Pr = 0.71$, $Bi = 1$, $P = 1$, $\eta = 1$, $\omega = 0$, $\varepsilon = 1$, $\Gamma = 1$ and $\phi = 90^\circ$.

the x_1 and x_2 directions, respectively, $\sigma = \sigma_r + i\sigma_i$ is the growth rate of the disturbances. The basic state, with respect to the infinitesimal disturbances, is said to be unstable if σ_r is greater than zero or stable if σ_r is less than zero. At the neutral state σ_r is equal to zero.

Substituting (18) into (14)–(17) then eliminating U , V and P , the equations describing the magnitudes of the disturbances can be obtained:

$$\left[(D^2 - k^2)^2 - \frac{ik_1 \bar{v}_1}{Pr} (D^2 - k^2) + \frac{ik_1 D^2 \bar{v}_1}{Pr} \right] W - Ra(ik_1 \sin \phi D + k^2 \cos \phi) \Theta = \frac{\sigma}{Pr} (D^2 - k^2) W \quad (19)$$

$$-(D\bar{\theta})W + (D^2 - k^2 - ik_1 \bar{v}_1 - 4\eta\tau P)\Theta + \eta\tau J = \sigma\Theta \quad (20)$$

$$\frac{12\tau^2}{1-\omega} P\Theta + \left(D^2 - k^2 - \frac{3\tau^2}{1-\omega} \right) J = 0 \quad (21)$$

where $D = d/dx_3$ and $k^2 = k_1^2 + k_2^2$. The associated boundary conditions are:

At $x_3 = 0$:

$$W = DW = 0 \quad (22a)$$

$$D\Theta + \frac{\eta(1-\omega)}{3\tau} DJ = 0 \quad (22b)$$

$$4P\Theta + \frac{\eta(1-\omega)}{3\tau\gamma_1} DJ - J = 0, \quad (22c)$$

At $x_3 = 1$:

$$W = DW = 0 \quad (22d)$$

$$D\Theta + Bi\Theta = 0 \quad (22e)$$

$$\frac{\eta(1-\omega)}{3\tau\gamma_2} DJ + J = 0. \quad (22f)$$

Equations (19)–(21) with the homogeneous boundary conditions (22) constitute a differential eigenvalue problem. For the existence of nontrivial solutions, the eigenvalues σ are of infinitely many discrete values and dependent on the parameters and the wavenumbers functionally as

$$\sigma = \sigma(\phi, Ra, Pr, Bi, P, \eta, \tau, \omega, \varepsilon, \Gamma, k_1, k_2). \quad (23)$$

It was found [11, 15] that the onset of instability in an inclined slot may either occur as stationary convective cells or in the form of travelling waves. At small inclination angles, two-dimensional longitudinal rolls with $k_1 = 0$ occur in the stationary manner. $Ra \cos \phi$ appears in the governing equations as the only term involving the inclination angle. In the meantime, both the real and imaginary parts of the eigenvalues vanish at the neutral state. In this situation, $Ra \cos \phi$ instead of σ may be considered to

be the eigenvalue. The Rayleigh number at the neutral state is independent of the Prandtl number,

$$Ra \cos \phi = f(Bi, P, \eta, \tau, \omega, \varepsilon, \Gamma, k_2). \quad (24)$$

When the inclination angle is greater than a transition angle ϕ_1 , instability due to two-dimensional transverse disturbances with $k_2 = 0$ occurs in the form of travelling waves. Under this condition, the Rayleigh number at the neutral state has to be searched until the real part of the most unstable eigenvalue vanishes. The imaginary part provides the information of the speed of propagation of disturbances, which is equal to $-\sigma_i/k_1$.

The perturbed complex stream function at the neutral state can be obtained by integrating v_3 with respect to x_2

$$\psi = -\frac{W}{ik_2} e^{ik_2 x}$$

for the longitudinal rolls, or with respect to x_1

$$\psi = -\frac{W}{ik_1} e^{i(k_1 x_1 + \sigma_i t)}$$

for the transverse rolls. For both cases, either the real part or the imaginary part can be employed to calculate the perturbed streamlines.

METHOD OF SOLUTION

The eigensystem (19)–(22) may be solved in many different ways. In the present analysis, the Chebyshev pseudospectral method [16] is used because of its high accuracy.

The n th-degree Chebyshev polynomial of the first kind [17] is defined by

$$T_n(\zeta) = \cos(n \cos^{-1} \zeta)$$

in the interval $\zeta \in [-1, 1]$. To fit the domain of definition of Chebyshev polynomials, the domain of the present problem is transformed from $0 \leq x_3 \leq 1$ to $-1 \leq \zeta \leq 1$ by $\zeta = 2(x_3 - 1/2)$.

The variables in equations (19)–(21) can be expanded as

$$W = \sum_{n=2}^{N+1} a_n \left\{ T_n - \frac{1}{2}[1 - (-1)^n]T_1 - \frac{1}{2}[1 + (-1)^n]T_0 \right\} \quad (25)$$

$$\Theta = \sum_{n=0}^{N-1} b_n T_n \quad (26)$$

$$J = \sum_{n=0}^{N-1} c_n T_n \quad (27)$$

where a_n , b_n and c_n are unknown coefficients. Theoretically the variables can be expanded by the basis functions, which are combinations of Chebyshev polynomials and fulfill all boundary conditions in equation (22). But because of the mixed boundary conditions of Θ and J , these basis functions are difficult to obtain. Therefore the basis functions are

Table 1. Ra_c and σ_i vs N at $\phi = 90^\circ$ for $Pr = 0.71$, $Bi = 1$, $P = 1$, $\eta = 1$, $\tau = 1$, $\omega = 0$, $\varepsilon = 1$, $\Gamma = 1$ and $k_c = 2.78$

N	10	12	14	16	18	20	22	24
Ra_c	43 181.41	43 304.67	43 202.54	43 195.80	43 192.94	43 193.29	43 193.22	43 193.22
σ_i	14.517	15.220	15.318	15.323	15.322	15.322	15.322	15.322

chosen such that only $W = 0$ at $\zeta = \pm 1$ are satisfied. Two boundary conditions for each variable then remain and must be treated later. Leaving the same number of boundary conditions for each variable makes for easy programming when the differential eigensystem is converted to an algebraic eigensystem.

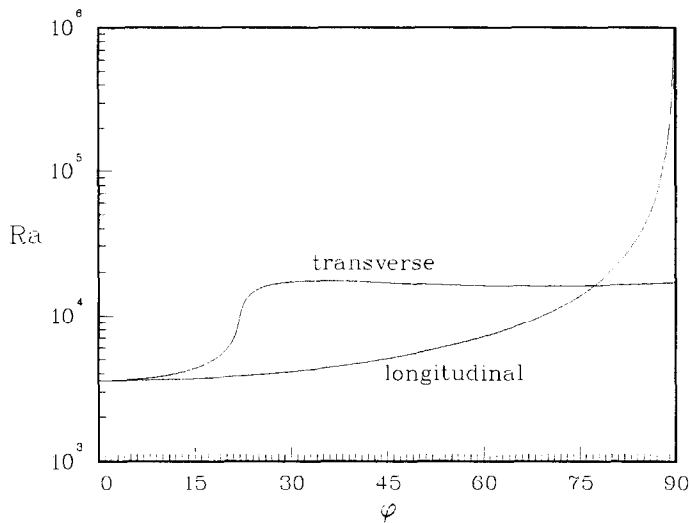
Substituting equations (25)–(27) into equations (19)–(21) and requesting the identities to hold at the $N-2$ collocation points,

$$\zeta_n = \cos\left(\frac{n}{N-1}\right)\pi \quad n = 1, 2, \dots, N-2,$$

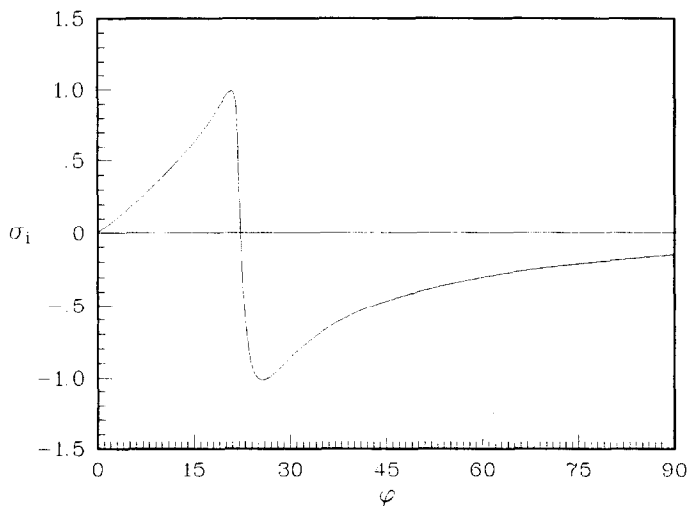
and at the two boundary conditions for each variable, an algebraic eigensystem is obtained :

$$AX = \sigma BX \tag{28}$$

where A and B are two $3N \times 3N$ coefficient matrices,



(a)



(b)

FIG. 3. (a) Rayleigh number and (b) σ_i at the neutral states vs inclination angle for $Pr = 0.71$, $Bi = 1$, $P = 1$, $\eta = 1$, $\tau = 0.001$, $\omega = 0$, $\varepsilon = 1$ and $\Gamma = 1$.

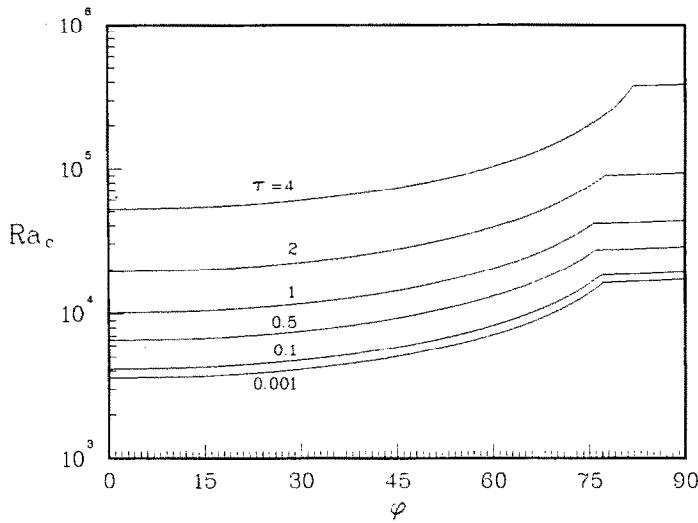


FIG. 4. The critical Rayleigh number vs inclination angle for different optical thicknesses at $Pr = 0.71$, $Bi = 1$, $P = 1$, $\eta = 1$, $\omega = 0$, $\varepsilon = 1$ and $\Gamma = 1$.

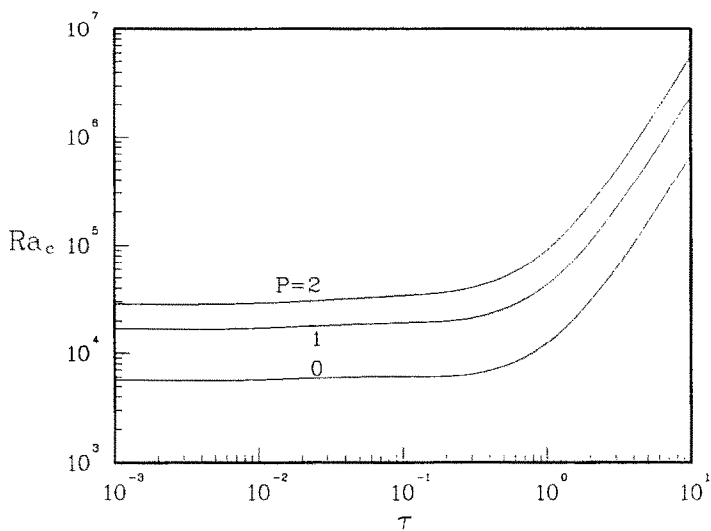


FIG. 5. Critical Rayleigh number vs optical thickness for $Pr = 0.71$, $Bi = 1$, $P = 1$, $\eta = 1$, $\tau = 1$, $\omega = 0$, $\varepsilon = 1$, $\Gamma = 1$ and $\phi = 90^\circ$.

and X is a $3N$ vector composed of the unknown coefficients.

The eigenvalues of the generalized eigensystem (28) can be solved directly by the QZ algorithm [18]. The Ra at the neutral state, at which the real part of the most unstable eigenvalue vanishes, is searched by the method of *regula falsi*. The iteration is not terminated until the real part of the most unstable eigenvalue is less than 10^{-6} or the difference of two consecutive Rayleigh numbers is less than 1. When longitudinal rolls occur at the onset of instability, σ is set to zero and $Ra \cos \phi$ is treated to be the eigenvalue. For the fixed parameters, different Ra at neutrally stable states may be obtained for different wavenumbers. The minimum Rayleigh number is the critical Rayleigh number

and denoted by Ra_c which occurs at the critical wavenumber k_c .

RESULTS AND DISCUSSION

The case of a horizontal layer with solid lower boundary and free upper boundary has been considered by Yang [13]. The results show that decreasing the transmissivity of the upper boundary has a stabilizing effect because less radiant energy can enter the flow. Decreasing the emissivity of the lower boundary decreases the energy absorbed by the lower boundary and develops a smaller temperature gradient, which in turn increases the stability. For the inclined slot, the same phenomena can be found. Therefore, the

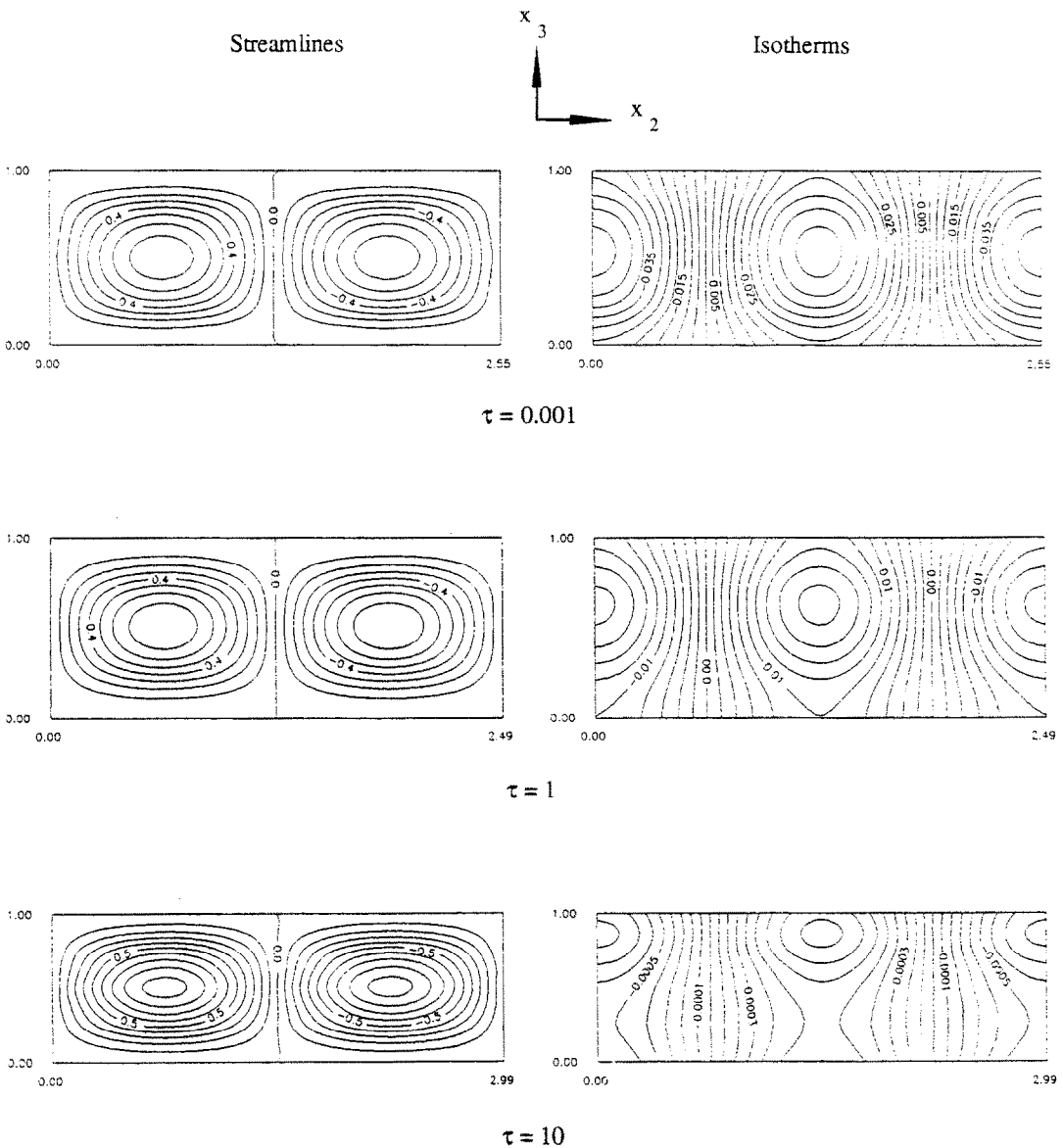


FIG. 6. Perturbed streamlines and isotherms of longitudinal rolls at $\phi = 0^\circ$ for $Pr = 0.71$, $Bi = 1$, $P = 1$, $\eta = 1$, $\omega = 0$, $\epsilon = 1$ and $\Gamma = 1$.

effects of transmissivity of the upper boundary and emissivity of the lower boundary are no longer examined but set equal to unity in the following presentation. Also for simplifying the analyses, the effects of the parameters η and ω on the stability of flow, which were discussed in refs. [10, 11, 14], are not considered in this study. They are respectively set equal to 1 and 0, which means that the fluids are assumed to be gray and nonscattering. Since most flow problems with pronounced effects of radiation are associated with gaseous media, the Prandtl number is set equal to 0.71 in the following calculations.

An accuracy test of the numerical results is exam-

ined and the dependence of Ra_c and σ_i is shown in Table 1 for the case that instability occurs as transverse rolls for $Bi = 1$, $P = 1$, $\tau = 1$ and $\phi = 90^\circ$. It is seen that for $N > 16$ convergent results for both Ra_c and σ_i have been obtained in this case. For the other cases for which Ra_c is greater or smaller, more or fewer terms should be employed. When the instability occurs as longitudinal rolls, since the result can be obtained from the relation $Ra_c = Ra_0/\cos \phi$, where Ra_0 is the critical Rayleigh number for $\phi = 0^\circ$, calculation is done only for the horizontal case for which fewer terms are usually enough.

For the horizontal case of an inclined slot, insta-

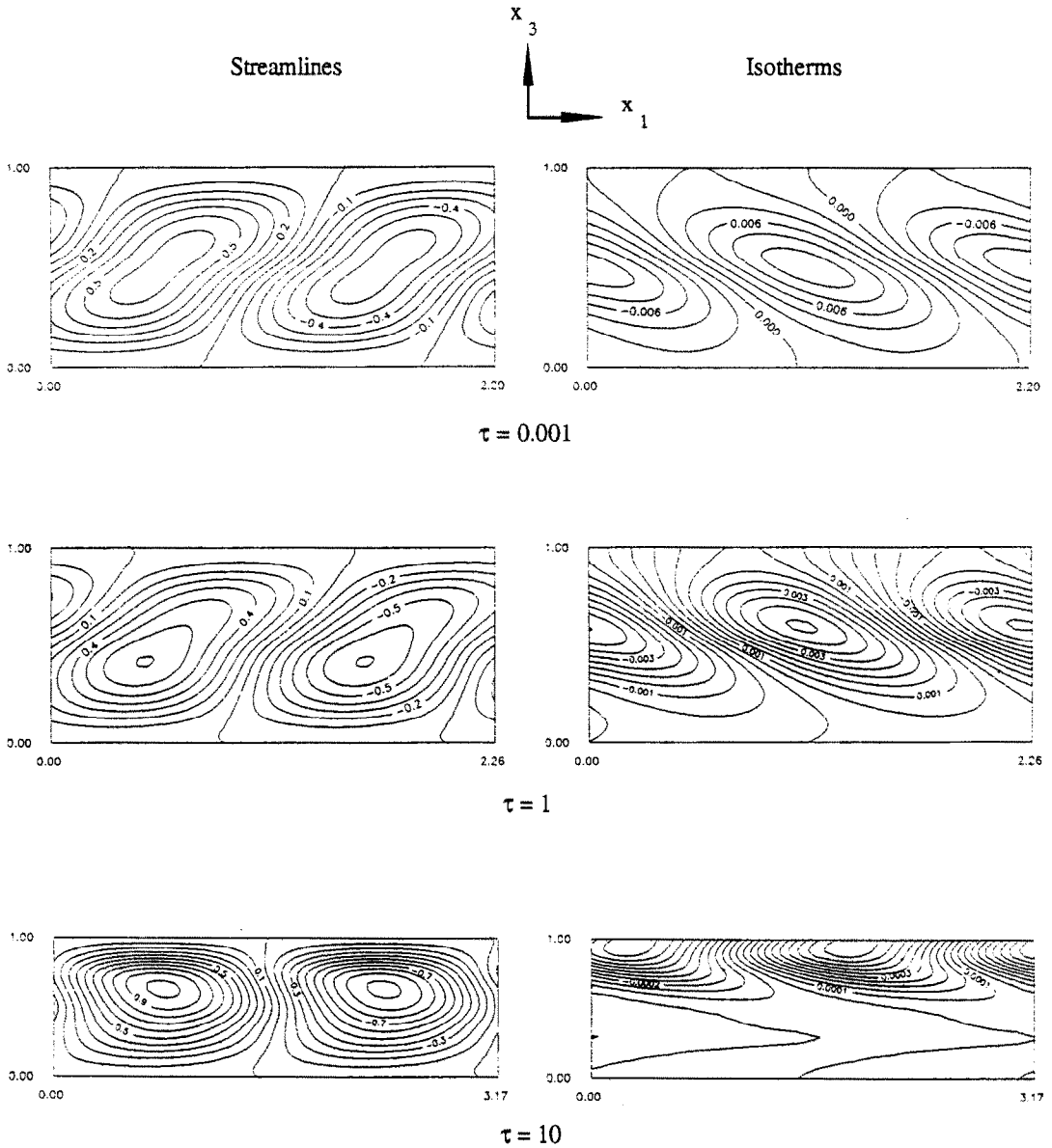


FIG. 7. Perturbed streamlines and isotherms of transverse rolls at $\phi = 90^\circ$ for $Pr = 0.71$, $Bi = 1$, $P = 1$, $\eta = 1$, $\omega = 0$, $\epsilon = 1$ and $\Gamma = 1$.

bility occurs as steady rolls. There is no difference for longitudinal or transverse rolls. When the inclination angle is increased from 0° , the buoyancy forces dominate the instability and steady longitudinal rolls still appear. After the inclination angle is greater than a transition angle, inertia forces rather than buoyancy forces dominate the instability. Transverse rolls then compete for occurrence. Figure 3(a) shows the Rayleigh number at the neutrally stable states corresponding to the onset of longitudinal rolls and transverse rolls vs inclination angle for an optically thin fluid at $Bi = 1$, $P = 1$ and $\tau = 0.001$. Basically, the

curves are similar to those of an inclined slot with different boundary temperatures, but now the transition angle is seen to be 77° which is larger than the transition angle 72° of the inclined slot with different boundary temperatures [11]. The imaginary part of the most unstable eigenvalue vs inclination angle is shown in Fig. 3(b). For longitudinal rolls, σ_i is always equal to zero which is represented by the horizontal line. When transverse rolls occur for $\phi > 0^\circ$, because of the asymmetric basic velocity and temperature profiles, the disturbances are propagating in the form of travelling waves under which σ_i is not equal to zero.

Korpela *et al.* [5, 6] found that in the case of inclined slot with different temperatures σ_1 is equal to zero for $0.24 < Pr < 12.7$ and ϕ close to 90° . Vest and Arpaci [3] experimentally showed that stationary rolls exist at Ra above the critical value for air at $\phi = 90^\circ$. Lauriat and Desrayaud [15] showed that when asymmetric boundary conditions are present, instabilities set in as a single travelling wave whose moving direction is dependent on the emissivities of the bounding walls. However, the present study considers that irradiation is incident from one side and both boundaries are floating in temperature under which instability certainly would not set in as stationary roll for the transverse disturbances.

Korpela [6] found that the transition angle is affected by Prandtl number significantly for $Pr < 12.7$ and moderately for $Pr > 12.7$. In this study, the radiation effect is the main concern. The effect of optical thickness, one of the important parameters in radiation, on the transition angle can be seen from Fig. 4 in which the stability curves of critical Rayleigh number vs inclination angle for different optical thicknesses are shown. The transition angle decreases then increases with increasing optical thickness and has a minimum value at τ about 1. It is also seen that the critical Rayleigh number increases with increasing optical thickness for any inclination angle. Because the optical thickness represents the resistance of incident radiative energy to penetrate to the lower boundary, increasing optical thickness decreases the penetration which in turn increases the stability of flow. The increase of the critical Rayleigh number with optical thickness is much greater for $\tau > 1$ than that for $\tau < 1$, which is shown in Fig. 5 for the vertical slot.

Figure 6 shows the perturbed streamlines and isotherms of the longitudinal rolls at $\phi = 0^\circ$ for different optical thicknesses. Since the longitudinal rolls are stationary, the stream function and temperature are periodically antisymmetric and symmetric, respectively, in the x_2 -direction as shown. It is also seen that the maximum perturbed temperature shifts toward the upper surface as the optical thickness increases because the penetration depth of radiant energy is smaller for a larger optical thickness. When the slot is at the vertical position, instability occurs in the form of travelling waves and the flow becomes unsteady. The perturbed streamlines and isotherms at an instant are shown in Fig. 7 for different optical thicknesses. It is seen that the flow remains periodic but is no longer symmetric in the x_3 -direction.

CONCLUSION

The stability of flow induced by irradiation from the upper side in the conduction regime in an inclined slot is studied numerically by linear theory. The results show that the transition angle, a cross-over angle of the flow from the longitudinal rolls to the transverse rolls, is affected by the optical thickness and has a minimum at the optical thickness near unity. When

the inclination angle is less than the transition angle, instability sets in as stationary longitudinal rolls. When the inclination angle is greater than the transition angle, instability occurs in the form of travelling waves. However, increasing the radiation effects in the participating fluid, by increasing the optical thickness or the Planck number, increases the stability of the flow.

Acknowledgement—The authors would like to acknowledge the National Science Council, R.O.C. for its support of the present work through project NSC 79-0401-E009-13.

REFERENCES

1. G. Z. Gershuni, On the stability of plane convective motion of a fluid, *Zh. Tech. Fiz.* **23**, 1838–1844 (1953).
2. G. K. Batchelor, Heat transfer by free convection across a closed cavity between vertical boundaries at different temperatures, *Q. Appl. Math.* **12**, 209–233 (1954).
3. C. M. Vest and V. S. Arpaci, Stability of natural convection in a vertical slot, *J. Fluid Mech.* **36**, 1–15 (1969).
4. J. E. Hart, Stability of the flow in a differentially heated inclined box, *J. Fluid Mech.* **47**, 547–576 (1971).
5. S. A. Korpela, D. Gozum and C. B. Baxi, On the stability of the conduction regime of natural convection in a vertical slot, *Int. J. Heat Mass Transfer* **16**, 1683–1690 (1973).
6. S. A. Korpela, A study on the effect of Prandtl number on the stability of the conduction regime of natural convection in an inclined slot, *Int. J. Heat Mass Transfer* **17**, 215–222 (1974).
7. D. W. Ruth, K. G. T. Hollands and G. D. Raithby, On free convection experiments in inclined air layers heated from below, *J. Fluid Mech.* **96**, 461–479 (1980).
8. R. M. Clever and F. H. Busse, Instabilities of longitudinal convection rolls in an inclined layer, *J. Fluid Mech.* **81**, 107–127 (1977).
9. A. Chait and S. A. Korpela, The secondary flow and its stability for natural convection in a tall vertical enclosure, *J. Fluid Mech.* **200**, 189–216 (1989).
10. V. S. Arpaci and Y. Bayazitoglu, Thermal stability of radiating fluids: Asymmetric slot problem, *Phys. Fluids* **16**, 589–593 (1973).
11. M. A. Hassab and M. N. Ozisik, Effects of radiation and convective boundary conditions on the stability of fluid in an inclined slender slot, *Int. J. Heat Mass Transfer* **22**, 1095–1105 (1979).
12. B. W. Webb and R. Viskanta, Radiation-induced buoyancy-driven flow in rectangular enclosures: experiment and analysis, *J. Heat Transfer* **109**, 427–433 (1987).
13. W.-M. Yang, Thermal instability of a fluid layer induced by radiation, *Numerical Heat Transfer* **17**, 365–376 (1990).
14. V. S. Arpaci and D. Gozum, Thermal stability of radiating fluids: The Benard problem, *Phys. Fluids* **16**, 581–589 (1973).
15. G. Lauriat and G. Desrayaud, Influences of the boundary conditions and linearization on the stability of a radiating fluid in a vertical layer, *J. Heat Transfer* **28**, 1613–1617 (1985).
16. C. Canuto, M. Y. Hussaini, A. Quarteroni and T. A. Zang, *Spectral Methods in Fluid Dynamics*. Springer-Verlag, New York (1988).
17. L. Fox and I. B. Parker, *Chebyshev Polynomials in Numerical Analysis*. Oxford University Press, London (1968).
18. C. B. Moler and G. W. Stewart, An algorithm for generalized matrix eigenvalue problems, *SIAM J. Numer. Anal.* **10**, 241–256 (1973).